Research Article | Vol. 30, No. 19 / 12 Sep 2022 / Optics Express 33860
Optics EXPRESS

Reconstructing Gaussian bipartite states with a single polarization-sensitive homodyne detector

JONAS JUNKER,* DENNIS WILKEN, DANIEL STEINMEYER, AND MICHÈLE HEURS

Max Planck Institute for Gravitational Physics (Albert Einstein Institute), and Institute for Gravitational Physics, Leibniz Universität Hannover, Callinstraße 38, 30167 Hannover, Germany
jonas.junker@aei.mpg.de

Abstract: We present a novel method to fully estimate Gaussian bipartite polarization states using only a single homodyne detector. Our approach is based on [Phys. Rev. Lett. **102**, 020502 (2009)], but circumvents additional optics, and thereby losses, in the signal path. We provide an intuitive explanation of our scheme without needing to define auxiliary modes. With six independent measurements, we fully reconstruct the state's covariance matrix. We validate our method by comparing it to a conventional dual-homodyne measurement scheme.

1. Introduction

Bipartite Gaussian states increasingly gain importance as a reliable resource for numerous quantum technologies. The need for continuous-wave bipartite (entangled) states reaches from gravitational wave metrology [1,2] over quantum communication [3] including quantum teleportation [4,5] to quantum imaging [6,7]. For a full state characterization, the covariance matrix of the bipartite state needs to be measured. It contains the complete entanglement information and, therefore, allows to determine the quality of the state.

To reconstruct the covariance matrix of a bipartite Gaussian state, usually a homodyne measurement is performed. The measurement process destroys the optical quantum state and, in return, provides information needed to reconstruct the covariance matrix of the state. Any quantum decoherence arising before (e.g., due to lossy optics) or during the detection process (e.g., due to non-unitary detection efficiency) will degrade the reconstruction fidelity and should be avoided.

We consider Gaussian two-mode squeezed states where for specific combinations of quadratures the noise is reduced below the classical limit. Traditionally, these states are detected with a dual-homodyne scheme, which effectively measures both modes individually before the signals are electrically combined [8–11]. However, the full covariance matrix can also be obtained by using only a single homodyne detector (HD) [12,13]. The method demonstrated in [14] requires the measurement of additionally defined modes which need to be detected in a series of different measurements. In [14] the detection scheme itself inherently introduces decoherence. The two-mode squeezed state needs to pass through up to three additional optical components, introducing optical loss, even though on a small scale, degrading the bipartite state's quality before its detection.

In this letter, we present an advanced single-homodyne detection scheme to reconstruct the full covariance matrix of a two-mode squeezed state generated by a polarization-non-degenerate optical parametric oscillator (NDOPO). To measure variances of different combinations of quadratures, our technique requires six measurements with differently polarized local oscillators. We provide an intuitive explanation of our scheme. Compared to [14], the state under consideration does not pass three additional optics, typically introducing an optical loss of about 0.5 %. Thus, our state deteriorates less on the way to the detection, avoiding decoherence. While this effect is small for currently achieved polarization bipartite states, it becomes relevant once two-mode

#465186 https://doi.org/10.1364/OE.465186
Journal © 2022 Received 25 May 2022; revised 3 Jul 2022; accepted 27 Jul 2022; published 31 Aug 2022

Optics EXPRESS

squeezing levels reach performance of the current single-mode squeezers [15]. In addition, we were able to reduce the number of required optical components. With our measurement, we show that the estimated two-mode squeezed state fulfills the Duan criterion [16] and the Reid criterion [17] demonstrating the Einstein-Podolsky-Rosen (EPR) paradox. To confirm our method, we compare our results to a measurement with a conventional dual-homodyne scheme.

2. Theoretical background

We consider bipartite two-mode squeezed Gaussian states with s- and p-polarized non-degenerate modes a_s and a_p. The state is described by a set of canonical operators $\mathbf{X} = (x_1^\mathrm{s}, x_2^\mathrm{s}, x_1^\mathrm{p}, x_2^\mathrm{p})$, with amplitude quadratures $x_1^\mathrm{j} = (a_\mathrm{j} + a_\mathrm{j}^\dagger)$ and phase quadratures $x_2^\mathrm{j} = i(a_\mathrm{j} - a_\mathrm{j}^\dagger)$ with $\mathrm{j} = \{s, p\}$. An arbitrary quadrature operator measured in a reference system rotated by α can be written as $x_\alpha^\mathrm{j} = x_1^\mathrm{j} \cos\alpha + x_2^\mathrm{j} \sin\alpha$.

Gaussian states are fully characterized by their first and second moments [18]. The first moments $\boldsymbol{d}$ are defined as $d_\mathrm{k} = \langle X_\mathrm{k} \rangle$ and vanish for undisplaced states, e.g. for squeezed vacuum. The second moments are represented in the covariance matrix $\boldsymbol{\sigma}$ and contain the full information about the (quantum) noise and the entanglement. The covariance matrix is a real symmetric positive matrix defined as

$$\boldsymbol{\sigma} = \begin{pmatrix} \mathrm{var}\, x_1^\mathrm{s} & \mathrm{cov}\, x_1^\mathrm{s}, x_2^\mathrm{s} & \mathrm{cov}\, x_1^\mathrm{s}, x_1^\mathrm{p} & \mathrm{cov}\, x_1^\mathrm{s}, x_2^\mathrm{p} \\ \mathrm{cov}\, x_2^\mathrm{s}, x_1^\mathrm{s} & \mathrm{var}\, x_2^\mathrm{s} & \mathrm{cov}\, x_2^\mathrm{s}, x_1^\mathrm{p} & \mathrm{cov}\, x_2^\mathrm{s}, x_2^\mathrm{p} \\ \mathrm{cov}\, x_1^\mathrm{p}, x_1^\mathrm{s} & \mathrm{cov}\, x_1^\mathrm{p}, x_2^\mathrm{s} & \mathrm{var}\, x_1^\mathrm{p} & \mathrm{cov}\, x_1^\mathrm{p}, x_2^\mathrm{p} \\ \mathrm{cov}\, x_2^\mathrm{p}, x_1^\mathrm{s} & \mathrm{cov}\, x_2^\mathrm{p}, x_2^\mathrm{s} & \mathrm{cov}\, x_2^\mathrm{p}, x_1^\mathrm{p} & \mathrm{var}\, x_2^\mathrm{p} \end{pmatrix}. \tag{1}$$

For a coherent state all covariances (the off-diagonal elements) vanish and the covariance matrix has a diagonal form with $\boldsymbol{\sigma} = \mathrm{diag}(1, 1, 1, 1)$. For a polarization two-mode squeezed state the covariance matrix is not diagonal due to correlations between the quadratures. Instead of squeezing, an amplified noise will be visible when looking only at variances of single quadratures. However, we measure squeezing in the combined quadrature variances, e.g. var $(x_1^\mathrm{s} \pm x_1^\mathrm{p})$ and var $(x_2^\mathrm{s} \pm x_2^\mathrm{p})$. These combined variances are connected via the identity

$$\mathrm{var}\, x_\mathrm{i} \pm x_\mathrm{j} = \mathrm{var}\, x_\mathrm{i} + \mathrm{var}\, x_\mathrm{j} \pm 2\, \mathrm{cov}\, x_\mathrm{i}, x_\mathrm{j} \tag{2}$$

to the covariance matrix with $\sigma_{i,k} = \mathrm{cov}\, x_i, x_j$. The covariance matrix of any N-mode Gaussian state can be visualized by the Wigner function [19] defined as in [20]

$$W(\boldsymbol{X}) = \frac{1}{\pi^N \sqrt{\det(\boldsymbol{\sigma})}} e^{-(\boldsymbol{X}-\boldsymbol{d})^\top \sigma^{-1} (\boldsymbol{X}-\boldsymbol{d})}. \tag{3}$$

3. Reconstruction method

Homodyne detection is a standard technique to quantify the noise of a quantum state. In a balanced homodyne detection, see Fig. 1, the signal mode a is sent onto a 50/50 beam splitter where it interferes with a strong local oscillator (LO). The two output fields of the beam splitter are detected on two individual photodiodes. The photocurrents are subtracted and converted into a voltage Δu that is monitored on a spectrum analyzer. The part of mode a to be measured is selected by the specific mode characteristics of the LO b (such as spatial mode shape and polarization), as only the projection of a onto b interferes with b and is amplified by b to detectable powers. Changes in the local oscillator's characteristics thus lead to detecting different parts of mode a. This is an important insight towards understanding the detection scheme. Considering

Optics EXPRESS

single-mode fields, the detection phase determines the measured readout quadrature, e.g., phase or amplitude quadrature.

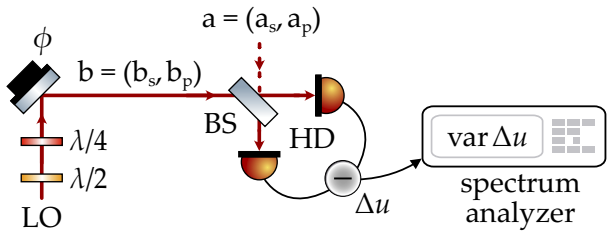

Fig. 1. Basic setup of our single HD reconstruction method. The LO is transmitted by a half-wave and a quarter-wave plate and experiences a phase shift ϕ. Then, the orthogonal polarization contributions of the LO b_s and b_p interfere with the corresponding fields of the signal a_s and a_b on a 50/50 beam splitter. The powers are measured on a HD where the difference voltage Δu is sent to a spectrum analyzer to quantify its variance. BS: 50/50 beam splitter, LO: local oscillator, HD: homodyne detector

For a polarization non-degenerate two-mode field, the readout quadrature combination can be determined by changing the magnitude and phase of the s-pol and p-polarization component of the LO, namely by adjusting its polarization. We now need to find the local oscillator's polarization states required to gain full knowledge of the covariance matrix described in (1). With a purely s-polarized LO $b = (b_\mathrm{s}, 0)$, the detection scheme is only sensitive to the s-polarized part of the signal beam. A LO with s- and p- polarization components $b = (b_\mathrm{s}, b_\mathrm{s})$ measures different linear combinations of the two modes a_s and a_p, depending on the phase difference of the LO modes b_s and b_p. In this sense, the single HD can also be interpreted as two independent HD detectors separated in polarization, sharing the same photodiodes.

As we will show in the following, six measurements with the below polarization states of the LO are sufficient to reconstruct the covariance matrix.

$$\text{linear p:} \quad b_\mathrm{lp} = (0, b) \quad \text{for var } x^\mathrm{p}_\phi \tag{4a}$$

$$\text{linear s:} \quad b_\mathrm{ls} = (b, 0) \quad \text{for var } x^\mathrm{s}_\phi \tag{4b}$$

$$\text{diagonal} + \pi/4: \quad b_\mathrm{lr} = b/\sqrt{2}\,(1, 1) \quad \text{for var } (x^\mathrm{p}_\phi + x^\mathrm{s}_\phi) \tag{4c}$$

$$\text{diagonal} - \pi/4: \quad b_\mathrm{ll} = b/\sqrt{2}\,(-1, 1) \quad \text{for var } (x^\mathrm{p}_\phi - x^\mathrm{s}_\phi) \tag{4d}$$

$$\text{left circular:} \quad b_\mathrm{cl} = b/\sqrt{2}\,(1, i) \quad \text{for var } (x^\mathrm{p}_\phi - x^\mathrm{s}_{\phi+\pi/2}) \tag{4e}$$

$$\text{right circular:} \quad b_\mathrm{cr} = b/\sqrt{2}\,(1, -i) \quad \text{for var } (x^\mathrm{p}_\phi + x^\mathrm{s}_{\phi+\pi/2}). \tag{4f}$$

For the calculation, we decompose the field operators a and b in a constant and a fluctuating term: $a = \langle a \rangle + \delta a$ and $b = \langle b \rangle + \delta b$. Since the LO is much more intense than the signal with $\langle b \rangle \gg \langle a \rangle$ we neglect $\langle a \rangle$ terms as well as all higher-order δ^2 terms. Finally, we compute the variance of the difference voltage var Δu of the homodyne detection that is later monitored by a spectrum analyzer.

First, we consider the case when the LO is in a linear s- or p-polarized state, see Eqs. (4a, 4b). For a p-polarized LO we find var Δu = var x^p_ϕ, and for an s-polarized LO, var Δu = var x^s_ϕ. For the specific phases $\phi = 0$ and $\phi = \pi/2$, we obtain the four main diagonal elements $\sigma_{i,i}$ of the covariance matrix. When we set the local oscillators phase to $\phi = \pi/4$ and again measure var Δu,

Optics EXPRESS

we can compute the $\sigma_{1,2} = \sigma_{2,1}$ and $\sigma_{3,4} = \sigma_{4,3}$ entries of the covariance matrix by using our already reconstructed main diagonal entries of the covariance matrix and the identity [21]

$$\text{var}\, x^{\text{j}}_{\phi=\pi/4} = \frac{1}{2}\left(\text{var}\, x^{\text{j}}_1 + \text{var}\, x^{\text{j}}_2 + 2\,\text{cov}\, x^{\text{j}}_1, x^{\text{j}}_2\right). \tag{5}$$

Following this procedure, the first six independent entries (in (1) in red dotted) of the covariance matrix can be obtained.

Second, we prepare the LO in a $\pm\pi/4$ linearly rotated polarization state, see Eqs. (4c, 4d). We measure the sum (difference) of amplitude or phase quadratures of both contributing modes, which is given by $\text{var}\,\Delta u = \text{var}\, x^{\text{p}}_{\phi} \pm x^{\text{s}}_{\phi}$. This is an elegant method to directly detect the sum (difference) of the same quadrature of modes with orthogonal polarizations. Now, the detector simultaneously detects the s- and p-polarized contributions and thus directly adds the quadratures. We can compute the $\sigma_{1,3} = \sigma_{3,1}$ and the $\sigma_{2,4} = \sigma_{4,2}$ entries by taking the main diagonal entries of the covariance matrix and (2). This procedure results in two more independent entries of the covariance matrix (in (1) in green solid).

Third and lastly, we prepare the LO in a right (left) circular polarized state, see Eqs. (4e, 4f). Now, mixing between quadratures and polarization modes occurs, which can be seen by $\text{var}\,\Delta u = \text{var}\,(x^{\text{p}}_{\phi} \pm x^{\text{s}}_{\phi+\pi/2})$. To compute the missing $\sigma_{1,4} = \sigma_{4,1}$ and $\sigma_{2,3} = \sigma_{3,2}$ entries, we again use the main diagonal elements from the first part and the identity from (2). This way, the last two independent entries (in (1) in blue dashed) are obtained, leading to a fully reconstructed covariance matrix.

4. Experimental setup

The measured two-mode squeezed state is generated by a polarization non-degenerate optical parametric oscillator (NDOPO) as shown in Fig. 2. The NDOPO is similar to the (OPO) presented in [22]. It consists of an input/output mirror with power reflectivity of $R_{\text{in}} = 0.95$ and three highly-reflective mirrors for the fundamental wavelength 1064 nm. The cavity is kept on resonance for 1064 nm by applying the Pound-Drever-Hall technique (not shown in Fig. 2). We measured the cavity linewidth to be 1.7 MHz. The optical round-trip length of the cavity is 1.522 m, which leads to a free spectral range of 197.0 MHz.

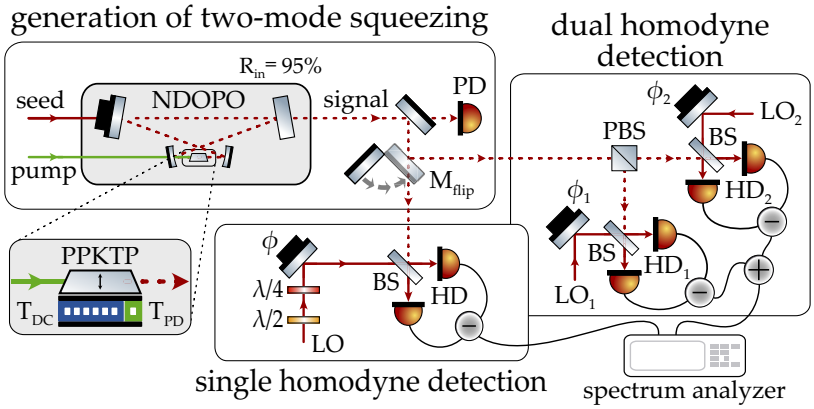

Fig. 2. Experimental setup consisting of generation and detection stage. We either detect the two-mode squeezed state with a single HD (bottom box) or, using the flipping mirror M_{flip}, with a dual HD. NDOPO: non-degenerate optical parametric oscillator, PD: photo detector, M: mirror, PBS: polarizing beam splitter, BS: 50/50 beam splitter, LO: local oscillator, HD: homodyne detector.

Optics EXPRESS

The core element of the NDOPO is a 1 mm × 2 mm × 10 mm (PPKTP) crystal for the non-linear type II down-conversion process, see Fig. 2. The optimal phase-matching condition for the down-conversion process is ensured by temperature controlling the larger left (8 mm) part of the crystal to $T_{DC} = 30^{\circ}$c. Since the birefringent crystal is wedged, we can roughly adjust the degeneracy point of the two polarization resonances by carefully shifting it perpendicularly to the cavity beam axis and thus changing the optical path length inside the crystal. Fine-tuning of the degree of degeneracy can be achieved by changing the temperature $T_{PD} \approx T_{DC}$ of the right (2 mm) part of the crystal by less than $\pm 1^{\circ}$c. We inject 650 mW of 532 nm pump light in a single-pass configuration. The pump phase can be locked to a seed field by detecting its de-amplification on the photodiode PD as in [23]. Also shown in Fig. 2 is the detection scheme for the two-mode squeezed state. To reconstruct the covariance matrix we can either use the conventional dual homodyne scheme or measure the state with our approach based on a single HD.

5. Reconstruction results

In this section, we explain how we have taken the measurements and present and discuss our reconstructed covariance matrices. We can employ the conventional dual-homodyne approach by using the flipping mirror M_{flip} in Fig. 2. In this case, the s- and p-polarization contributions of the signal are split by a polarising beam splitter (PBS) and are detected by the two individual homodyne detectors HD_1 and HD_2. With mirrors clamped onto piezoelectric elements, we can change the two detection phases, respectively. By combining the voltages from both homodyne detectors for different phases ϕ_1 and ϕ_2 of the s-polarized LO_1 and the p-polarized LO_2, the covariance matrix can be reconstructed [8,11].

To utilize the single HD approach, we send the signal beam directly onto the HD. Here, the signal interferes with the LO, whose particular polarization state is prepared with a half-wave and a quarter wave-plate. We use the six differently polarized local oscillator fields to take our measurements as explained in Section 3. The polarization states are generated by using motorized pre-calibrated rotation mounts for the two waveplates. By tuning the piezoelectric element (PZT), we change the relative phase ϕ between the local oscillator and the two-mode squeezed state (signal), as depicted in Fig. 2. The difference voltage Δu of the HD is measured with a spectrum analyzer [Keysight, N9020A MXA], and the trace is plotted in Fig. 3. We have taken the measurements over a zero span at 197 MHz, which is the first free spectral range frequency of the NDOPO. The measurements are normalized to shot noise and the electronic dark noise (which was roughly 15 dB below the shot noise) is subtracted. Each colored trace shows the signal's noise for a specific polarization state of the LO. For a purely s- or p-polarized LO, we observe the thermal noise characteristic of the state. The marginal dependence on the phase ϕ is probably due to a remaining mismatch between polarization bases of signal and local oscillator. For the other four polarizations we observed a squeezed noise of $-6.7(2)$ dB and an anti-squeezed noise of 12.8(2) dB. Here, we took up to six data points for each required variance. Thus, we average over the measurement time of 0.8 s, to get a higher precision for the entries in the covariance matrix.

When using the dual-homodyne scheme to analyze the two-mode squeezed state, we obtain measurements similar to those as shown in Fig. 3. We measured the s-pol and p-polarization thermal states by using only one of the two homodyne detectors. If we monitor the combined signal behind an electronic adder [Mini-Circuits, ZFSC-2-5-S+], we obtain variances of different quadrature combinations. For each measurement, we locked the detection phase of one HD (e.g. ϕ_1 on HD_1) and ramped the other detection phase (ϕ_2). Following this procedure, we can also reconstruct the full covariance matrix of the same two-mode squeezed state.

The reconstructed covariance matrices for the single HD and dual HD schemes are shown in Fig. 4. The entries are average values calculated over the full measurement time. We found both covariance matrices exhibiting well-matching entries within the statistical measurement

Optics EXPRESS

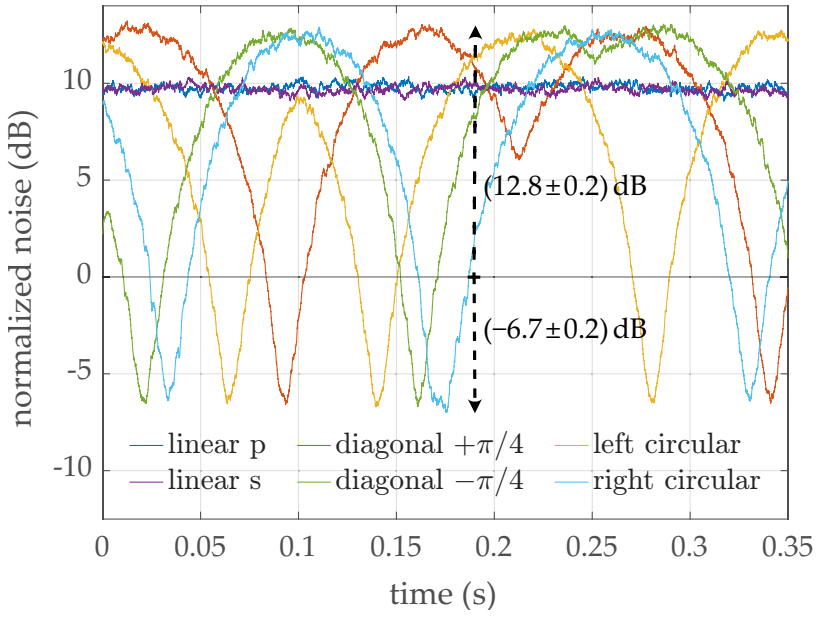

Fig. 3. Zero-span measurements taken with the single homodyne detector for six different polarization states of the local oscillator at 197 MHz, normalized on shot noise. We observe a squeezed level of −6.7 dB and an anti-squeezing level of 12.8 dB. Resolution bandwidth: 200 kHz, video bandwidth: 100 kHz.

uncertainties. For the main-diagonal entries, the standard deviation is at most 0.2, according to our statistics from taking several data points per trace. The uncertainty for the off-diagonal entries in the covariance matrix (CM) is up to a factor of 4 larger because they were indirectly obtained. In the following, we elaborate on the potential origins dominating the measurement uncertainties.

$$\text{single HD}\qquad \sigma = \begin{pmatrix} 9.0 & 0.0 & -9.2 & 0.0 \\ 0.0 & 9.5 & 0.0 & 9.2 \\ -9.2 & 0.0 & 9.8 & 0.0 \\ 0.0 & 9.2 & 0.0 & 9.3 \end{pmatrix} \qquad \text{dual HD}\qquad \sigma = \begin{pmatrix} 9.0 & -0.1 & -9.1 & -0.2 \\ -0.1 & 9.3 & -0.2 & 9.0 \\ -9.1 & -0.2 & 9.6 & 0.0 \\ -0.2 & 9.0 & 0.0 & 9.1 \end{pmatrix}$$

Fig. 4. Comparison of the reconstructed covariance matrices obtained from measurements with the single homodyne detector (left) and the dual homodyne detector (right) approach. We observe nearly identical results for both approaches.

Since our single-homodyne measurements work with a polarization-sensitive local oscillator, they require reliable polarization optics. The beam splitter should have an equal splitting ratio of 50/50 for both polarizations for a precise reconstruction. Usually, this can be realized with the appropriate coating and careful alignment of the angle of incidence. In our experiment we could achieve $R_s \approx R_p \approx 50\%$ with a precision of ±0.5%. Another important factor is the polarization accuracy of the LO and how well it matches the signal's polarization basis. The motorized rotations mounts [Thorlabs, ELL14] have an adjustment precision of ±0.3% to tune the ellipticity and rotation angle of the LO. The polarization was monitored by a polarimeter

Optics EXPRESS

[Thorlabs, PAX1000IR1]. However, these mentioned experimental uncertainties do not dominate the errors in the covariance matrix.

For the single-homodyne detection, the polarization state of the two-mode squeezed state is highly important when it interferes with the local oscillator at the beam splitter. Ideally, the two-mode squeezed state is diagonally linearly polarized. However, the polarization state changes due to any polarization non-degeneracy effects. One origin could be an asymmetric propagation phase for s- and p-polarization arising from mirror reflections, which is a static effect. Additionally, a slightly fluctuating resonance condition of the NDOPO for s- and p-polarization could also dynamically change their phase relation (the polarization state) but also their magnitudes (the squeezing degree). In our setup, this might be the case, most likely due to small temperature fluctuations in the crystal. This effect which originates from the NDOPO source and not from the detection scheme, dominates the uncertainties in the covariance matrices.

The comparison of both covariance matrices in Fig. 4 indicates that the state obtained by the dual HD method is slightly more squeezed. The main differences between the two detection setups are that, firstly, the propagation efficiencies for the three beam paths (to single HD vs. reflected at the PBS vs. transmitted at the PBS) are slightly different. Secondly, we measured slightly different visibilities (VIS) for the three homodyne detectors ($\mathrm{VIS_{1HD}} = 99\%$, $\mathrm{VIS_{2HD,s}} = 98\%$, $\mathrm{VIS_{2HD,p}} = 99\%$). However, these differences do not explain why the state detected with the dual HD method is slightly more squeezed. A better explanation is that the two-mode squeezed state becomes slightly elliptical polarized when it travels to the detector, as explained in the previous paragraph. A non-degrading elliptical polarized two-mode squeezed state is only a problem when using the single HD method.

We visualize the covariance matrix obtained from the single HD method in Fig. 5 by plotting the Wigner functions using Eq. (3) with $N = 1$. The Wigner functions $W(x_1^{\mathrm{s}}, x_1^{\mathrm{p}})$ and $W(x_2^{\mathrm{s}}, x_2^{\mathrm{p}})$ show squeezed states representing anti-correlated quadratures x_1^{s}, x_1^{p} and correlated quadratures x_2^{s}, x_2^{p}. These two Wigner functions are squeezed by a factor of 0.20 and 0.21, respectively. We observe thermal states for $W(x_1^{\mathrm{s}}, x_2^{\mathrm{s}})$ and $W(x_2^{\mathrm{p}}, x_1^{\mathrm{p}})$. Due to the strong similarity of the two covariance matrices, the Wigner functions for the dual HD case look nearly identical and are omitted here.

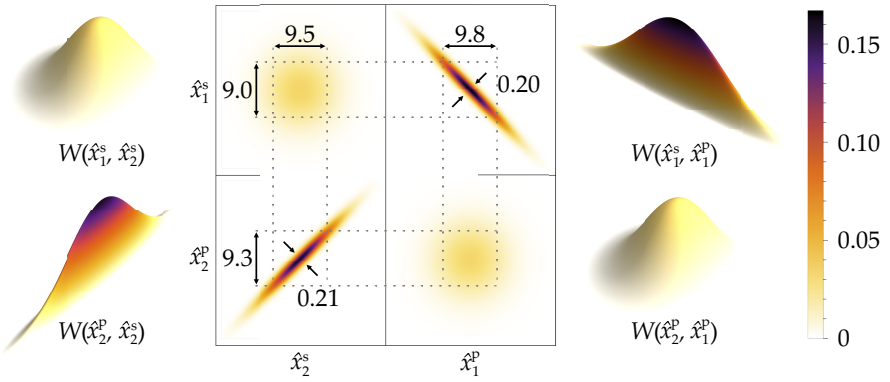

Fig. 5. Gaussian Wigner functions for different combinations of the four quadrature modes x_1^{p}, x_2^{p}, x_1^{s} and x_2^{s}. The distributions are plotted by using Eq. (1) and the reconstructed covariance matrix from our measurements with a single HD from Fig. 4.

To complete, we investigate our reconstructed two-mode squeezed state on inseparability and entanglement when we measure with a single HD. With our single HD approach, we can test these criteria directly, since we directly measure the required variances, see Section 3. We find a value of 0.42 ± 0.02 for the left hand side of the equation for the Duan

Optics EXPRESS

criterion var $(x_1^s + x_1^p)$ + var $(x_2^s - x_2^p)$<2 [16], falling a factor of roughly 4.8 below this criterion. The criterion from Reid can be seen as an inferred Heisenberg uncertainty relation with var $(x_1^s + x_1^p) \times$ var $(x_2^s - x_2^p)$<1 [17]. Using our reconstructed covariance matrix, the left hand side reads 0.044 ± 0.003, surpassing the Reid criterion by a factor of roughly 23, which clearly demonstrates the EPR paradox.

6. Discussion and conclusion

Finally, we discuss the drawbacks and the advantages of using our demonstrated single HD approach. The technical drawback of the single HD reconstruction method is its susceptibility to polarization inaccuracies. This applies for the beam splitter, which has to be equally reflective for s- and p-polarization, but also the matching of the polarization bases of LO and signal. Moreover, our scheme is sensitive to the actual phase delay between both fields, which potentially explains the slightly reduced squeezing values for the single HD measurements compared to those measured with the dual HD. However, our demonstrated method has some advantages compared to [14]. With the motorized rotation mounts, our measurements can be taken very fast. The most significant benefit is that we do not send the state under estimation through components other than the beam splitter, as this would introduce additional and unwanted decoherence. Typically, these losses are in the order of 0.5% for three optical components in transmission. They are small with respect to the total losses shown here. However, with increasing performance these losses become a more significant contribution to the loss budget - [15] showed a total loss of 2.5 % in a single-mode setup.

We have demonstrated a full Gaussian state estimation of a two-mode squeezed state by measurements with a single homodyne detector. Our detection scheme is similar to the method demonstrated in [14]. We use six different polarization states of the local oscillator, with each one measuring a particular combination of variances. These measurements allow us to fully reconstruct the covariance matrix of the two-mode squeezed state. The advantage of our method compared to [14] is that the state under estimation deteriorates less on the way to the homodyne detector because we avoid the transmission through of optical components (two waveplates and a polarising beam splitter), thereby retaining more coherence. To confirm our method, we compare our results to a measurement taken with a conventional dual-homodyne scheme. Our presented approach is an intuitive, low-loss alternative for characterizing bipartite polarization states.

Funding. Deutsche Forschungsgemeinschaft ((EXC 2122, Project ID 390833453), (EXC 2123, Project ID 390837967), (Project ID 239408513), Excellence PhoenixD, Excellence QuantumFrontiers, GRK 1991).

Disclosures. The authors declare no conflicts of interest.

Data availability. Data underlying the results presented in this paper are not publicly available at this time but may be obtained from the authors upon reasonable request.

References

1. Y. Ma, H. Miao, B. H. Pang, M. Evans, C. Zhao, J. Harms, R. Schnabel, and Y. Chen, "Proposal for gravitational-wave detection beyond the standard quantum limit through epr entanglement," Nat. Phys. **13**(8), 776–780 (2017).
2. J. Südbeck, S. Steinlechner, M. Korobko, and R. Schnabel, "Demonstration of interferometer enhancement through einstein–podolsky–rosen entanglement," Nat. Photonics **14**(4), 240–244 (2020).
3. N. Gisin and R. Thew, "Quantum communication," Nat. Photonics **1**(3), 165–171 (2007).
4. S. L. Braunstein and H. J. Kimble, "Teleportation of continuous quantum variables," Phys. Rev. Lett. **80**(4), 869–872 (1998).
5. D. Bouwmeester, J.-W. Pan, K. Mattle, M. Eibl, H. Weinfurter, and A. Zeilinger, "Experimental quantum teleportation," Nature **390**(6660), 575–579 (1997).
6. N. Treps, U. Andersen, B. Buchler, P. K. Lam, A. Maître, H.-A. Bachor, and C. Fabre, "Surpassing the standard quantum limit for optical imaging using nonclassical multimode light," Phys. Rev. Lett. **88**(20), 203601 (2002).
7. M. I. Kolobov and C. Fabre, "Quantum limits on optical resolution," Phys. Rev. Lett. **85**(18), 3789–3792 (2000).
8. J. DiGuglielmo, B. Hage, A. Franzen, J. Fiurášek, and R. Schnabel, "Experimental characterization of gaussian quantum-communication channels," Phys. Rev. A **76**(1), 012323 (2007).

Optics EXPRESS

9. Z. Y. Ou, S. F. Pereira, H. J. Kimble, and K. C. Peng, "Realization of the einstein-podolsky-rosen paradox for continuous variables," Phys. Rev. Lett. **68**(25), 3663–3666 (1992).
10. J. Laurat, G. Keller, J. A. Oliveira-Huguenin, C. Fabre, T. Coudreau, A. Serafini, G. Adesso, and F. Illuminati, "Entanglement of two-mode gaussian states: characterization and experimental production and manipulation," J. Opt. B: Quantum Semiclassical Opt. **7**(12), S577–S587 (2005).
11. S. Steinlechner, J. Bauchrowitz, T. Eberle, and R. Schnabel, "Strong einstein-podolsky-rosen steering with unconditional entangled states," Phys. Rev. A **87**(2), 022104 (2013).
12. V. D'Auria, A. Porzio, S. Solimeno, S. Olivares, and M. G. A. Paris, "Characterization of bipartite states using a single homodyne detector," J. Opt. B: Quantum Semiclassical Opt. **7**(12), S750–S753 (2005).
13. D. Steinmeyer, "Subsystems for all-optical coherent quantum-noise cancellation," Ph.D. thesis, Gottfried Wilhelm Leibniz Universität Hannover (2019).
14. V. D'Auria, S. Fornaro, A. Porzio, S. Solimeno, S. Olivares, and M. G. A. Paris, "Full characterization of gaussian bipartite entangled states by a single homodyne detector," Phys. Rev. Lett. **102**(2), 020502 (2009).
15. H. Vahlbruch, M. Mehmet, K. Danzmann, and R. Schnabel, "Detection of 15 db squeezed states of light and their application for the absolute calibration of photoelectric quantum efficiency," Phys. Rev. Lett. **117**(11), 110801 (2016).
16. L.-M. Duan, G. Giedke, J. I. Cirac, and P. Zoller, "Inseparability criterion for continuous variable systems," Phys. Rev. Lett. **84**(12), 2722–2725 (2000).
17. M. D. Reid, "Demonstration of the einstein-podolsky-rosen paradox using nondegenerate parametric amplification," Phys. Rev. A **40**(2), 913–923 (1989).
18. R. Simon, N. Mukunda, and B. Dutta, "Quantum-noise matrix for multimode systems: U(n) invariance, squeezing, and normal forms," Phys. Rev. A **49**(3), 1567–1583 (1994).
19. E. Wigner, "On the quantum correction for thermodynamic equilibrium," Phys. Rev. **40**(5), 749–759 (1932).
20. G. Adesso, S. Ragy, and A. R. Lee, "Continuous variable quantum information: Gaussian states and beyond," Open Syst. Inf. Dyn. **21**(01n02), 1440001 (2014).
21. V. Händchen, "Experimental analysis of Einstein-Podolsky-Rosen steering for quantum information applications," Ph.D. thesis, Gottfried Wilhelm Leibniz Universität Hannover (2016).
22. J. Junker, D. Wilken, N. Johny, D. Steinmeyer, and M. Heurs, "Frequency-dependent squeezing from a detuned squeezer," Phys. Rev. Lett. **129**, 033602 (2022).
23. J. Junker, D. Wilken, E. Huntington, and M. Heurs, "High-precision cavity spectroscopy using high-frequency squeezed light," Opt. Express **29**(4), 6053–6068 (2021).